

Viscoelastic Effects on the Phase Separation in Thermoplastics-Modified Epoxy Resin

Wenjun Gan, Yingfeng Yu, Minghai Wang, Qingsheng Tao, and Shanjun Li*

Department of Macromolecular Science and The Key Laboratory of Molecular Engineering of Polymer, Ministry of Education, Fudan University, Shanghai 200433, China

Received May 16, 2003; Revised Manuscript Received August 10, 2003

ABSTRACT: The phase separation of the diglycidyl ether of bisphenol A (DGEBA)/methyltetrahydrophthalic anhydride (MTHPA) blends modified with polyetherimide (PEI) in the presence of various amounts of accelerator benzyldimethylamine (BDMA) was investigated by scanning electron microscopy (SEM) and time-resolved light scattering (TRLS). The morphologies of the blends with the accelerator are of the co-continuous type, exhibiting irregular shapes. They are quite different from that without accelerator, in which the morphology is spherical. The TRLS results display clearly that the phase separation takes place according to a spinodal decomposition mechanism and the evolution of scattering vector q_m corresponding to epoxy droplets follows a Maxwell-type relaxation equation. The temperature-dependent relaxation time τ obtained for these blends can be described by the Williams–Landel–Ferry equation. It demonstrates experimentally that the coarsening processes of epoxy droplets and the final morphologies obtained in these thermoplastic–epoxy systems are affected by viscoelastic behavior.

1. Introduction

Over two decades, attempts have been made to modify epoxy resins with a high-performance engineering thermoplastic that has a high T_g and toughness, such as polysulfone (PSU),^{1,2} poly(ether sulfone) (PES),^{3–5} poly(ether ether ketone) (PEEK),⁶ and polyetherimide (PEI).^{7–9} As the thermoset precursor reacts, the entropy of mixing decreases with increasing molecular weight, and the Flory–Huggins interaction parameter changes very little (i.e., the enthalpy is nearly constant). According to the Flory–Huggins mean-field theory, as an average molecular weight of epoxy resin is reached where a homogeneous mixture is no longer favored, the thermoplastics-modified thermoset system separates into two phases.^{4,10} Different phase morphologies can be obtained, depending on the competition between the thermodynamics and kinetics of phase separation and the cross-linking chemical reaction, which are governed by the curing conditions, compositions, molecular weights, and molecular weight distributions of tougheners. The effective improvement in toughness is obtained only with the morphology structure of the co-continuous phase or phase inversion. In our previous work,^{11,12} a co-continuous phase structure was obtained in an epoxy resin modified with novel polyetherimide (PEI), and the fracture toughness was apparently improved. The process of phase separation was monitored with time-resolved light scattering (TRLS) and synchrotron radiation small-angle X-ray scattering (SR-SAXS), and it was suggested that the spinodal decomposition (SD) mechanism is most conceivable in thermoplastics-modified thermoset systems.

Recently, the viscoelastic phase separation of polymer blends has attracted increasing attention. Most of this attention has been focused on the binary or ternary system of thermoplastic–solvent or thermoplastic–thermoplastic such as PMMA (poly(methyl methacrylate))/PSAN (poly(styrene-co-acrylonitrile)),^{13,14} PS (polystyrene)/PVME,^{15–17} dextran/PEG (poly(ethylene glycol)/

H₂O),¹⁸ and PS (polystyrene)/PMPS (poly(methylphenylsiloxane)).¹⁹ As these thermoplastic–solvent or thermoplastic–thermoplastic systems are intensively investigated, a series of viscoelastic phase-separation theories are developed to interpret the phenomena taking place in the phase-separation process of the above systems. Tanaka first reported unusual phase separation caused by asymmetric molecular dynamics^{20,21} and found that viscoelastic phase separation was a universal phenomenon common to all dynamically asymmetric mixtures; the origin of the dynamic asymmetry might be caused by the size difference in component molecules of a mixture or the existence of another transition such as a glass transition.^{22,23} In these cases, domains of a fast dynamic phase appear in a slow dynamic phase matrix, and then networklike or spongelike structures are formed by the domain growth. Finally, a continuous slow dynamic phase develops into a dispersed phase by shrinkage. Therefore, even a minor polymeric component provides networklike continuous or co-continuous phase structures that brought about excellent mechanical properties. Zheng et al. found experimentally that the evolution of scattering intensity $I(t)$ and the temperature-dependent apparent diffusion coefficient $D_{app}(T)$ could be described by the WLF-like function.²⁴ Meanwhile, the dynamical asymmetry and viscoelastic effect are thought to play an important role in concentration fluctuations of polymer mixtures. A clarification of these effects is an important step toward a deeper understanding of the dynamics of concentration fluctuations in general complex fluid systems.^{25,26}

Although there is increasing interest in viscoelastic effect on the phase separation of polymer blends, there are few papers in the literature devoted to the discussion of viscoelastic effect on the phase separation of thermoplastic–thermoset systems. In the blend of epoxy resin modified with PEI, PEI has a high T_g of 217 °C; however, epoxy resin has a low T_g of about –5 °C. The T_g of a fully cured epoxy resin with methyltetrahydrophthalic anhydride (MTHPA) as the hardener will be about 110 °C,²⁷ which is much less than that of P-PEI.

* Corresponding author. E-mail: sjli@fudan.edu.cn.

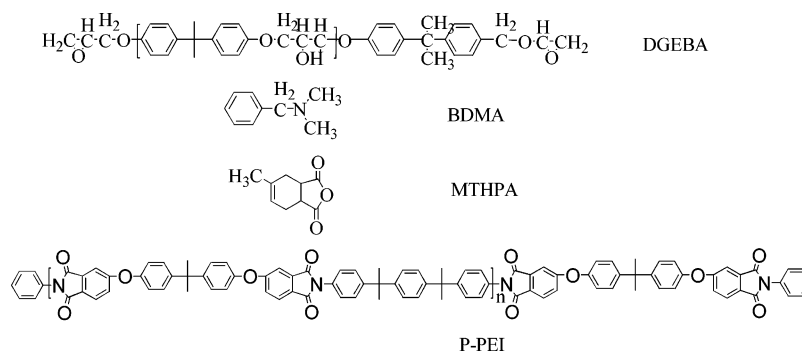


Figure 1. Chemical structures of epoxy resin (DGEBA), methyltetrahydrophthalic anhydride (MTHPA), accelerator (BDMA), and polyetherimide (P-PEI).

Table 1. Composition of Three Systems

	P-PEI (pbw)	MTHPA (pbw)	BDMA (pbw)
P720	20	80	0.2
HP720	20	80	0.1
NP720	20	80	0

Thus, the difference in the glass transition between the two components will accompany the entire phase separation. Obviously, this blend should be a dynamic asymmetry system in the relaxation and diffusion of segments, and phase separation would be influenced by the viscoelastic behavior.

The aim of the present work is to discuss the viscoelastic effects on the phase separation in the system of DGEBA/MTHPA modified with PEI. In these blends, various amounts of accelerator BDMA were used to change the curing rate of the blends because the quantity of the BDMA is quite little, hence the thermodynamic states of these blends could be considered to be approximately the same.

2. Experimental Section

2.1. Materials. A commercial epoxy resin (DER 332) from Dow Chemical, curing agent methyltetrahydrophthalic anhydride (MTHPA), and accelerator benzoyldimethylamine (BDMA) from the Shanghai Third Reagent Factory were used without further purification.

Polyetherimide (PEI) was synthesized from bisphenol A dianhydride (BISA-DA) and 4,4'-[1,4-phenylenebis(1-methylethylidene)]bis-aniline (BISP) in a stoichiometric ratio of 1:0.985 in *m*-cresol at 200 °C. After that, aniline was added to terminate the PEI, and the products were precipitated in alcohol and dried at 200 °C for about 4 hours. The polymer is designated as P-PEI, where P represents phenyl-terminated. The inherent viscosity of the P-PEI used here is 0.7 dL/g.

The chemical structures of DGEBA, BDMA, MTHPA, and polyetherimide are shown in Figure 1.

2.2. Sample Preparation. Epoxy blends containing 20 pbw (parts by weight) P-PEI were prepared by dissolving P-PEI in DGEBA at 150 °C. The mixture was cooled to 90 °C until a clear homogeneous solution was obtained, and a stoichiometric amount of cure agent MTHPA was added (with or without accelerator BDMA); then the blend was cooled rapidly to room temperature to avoid any further curing reaction. The compositions of modified systems involved in this work are listed in Table 1.

2.3. Time-Resolved Light-Scattering Measurements. The phase-separation process taking place during the isothermal curing reaction was observed in real time and in situ on the self-made time-resolved light scattering (TRLS) instrument with controllable hot chamber; the TRLS technique was described elsewhere.²⁸ The change in the light-scattering profiles was recorded at appropriate time intervals during isothermal curing. The sample for TRLS observation was prepared by melt-pressing a film with a thickness of about 20 μm.

2.4. Morphology Observation. The morphology of the isothermally cured resins was observed under a scanning electron microscope (SEM) (Philip XL 39). The samples were fractured in liquid nitrogen. All samples were coated with gold and mounted on copper mounts.

2.5. Glass-Transition Temperature (T_g) Measurement. Glass-transition temperature T_g was measured using a SETARAM differential scanning calorimeter (DSC-141). Small quantities of the samples (about 10 mg) were placed in hermetically sealed aluminum pans. The temperature was scanned from -70 to 20 °C at different heating rates. After the heat-flow curve was obtained, T_g was calculated with the program supplied by the SETARAM Corporation and is reported as the midpoint temperature of the glass transition.

3. Results and Discussion

3.1. Morphologies Observed by SEM. The morphologies of cured samples were observed with SEM. For all of the images presented here, the dark regions correspond to the epoxy-rich phase, and the bright regions correspond to the P-PEI-rich phase. As shown in Figure 2, the morphology of the P720 system consists of large P-PEI-rich domains, exhibiting irregular shapes and dispersed in an epoxy-rich continuous phase (Figure 2a) that is very close to the co-continuous-type phase structure. The morphology of the HP720 system (Figure 2b) is somewhat the same as Figure 2a. However, the NP720 system is spherical (Figure 2c), in which the P-PEI-rich phase is global and dispersed in the epoxy-rich continuous phase. SEM photographs of P-PEI-rich phases of the three systems are shown in Figure 2d-f. Obviously, different morphologies were observed despite the same initial P-PEI concentration.

3.2. Evolution of $I_m(t)$ and $q_m(t)$ during the Isothermal Process. Phase-separation processes of the three systems were traced in situ by TRLS. The change in the light-scattering profiles was recorded at appropriate time intervals during isothermal curing at 100, 110, 120, 130, 140, and 150 °C.

Figure 3a shows a typical example of the change in the scattering profile with demixing time t for the P720 system cured at 120 °C isothermally. Scattered-light intensity I is a function of time and scattering vector q ; the latter is defined by eq 1,

$$q = \left(\frac{4\pi}{\lambda} \right) \sin\left(\frac{\theta}{2}\right) \quad (1)$$

where λ is the wavelength of light in the sample and θ is the scattering angle. From the light-scattering profiles, the peak scattering vector q_m corresponding to an instantaneous maximum scattering intensity I_m was obtained. It decreased with time, and the relative intensity of scattered light increased continually from

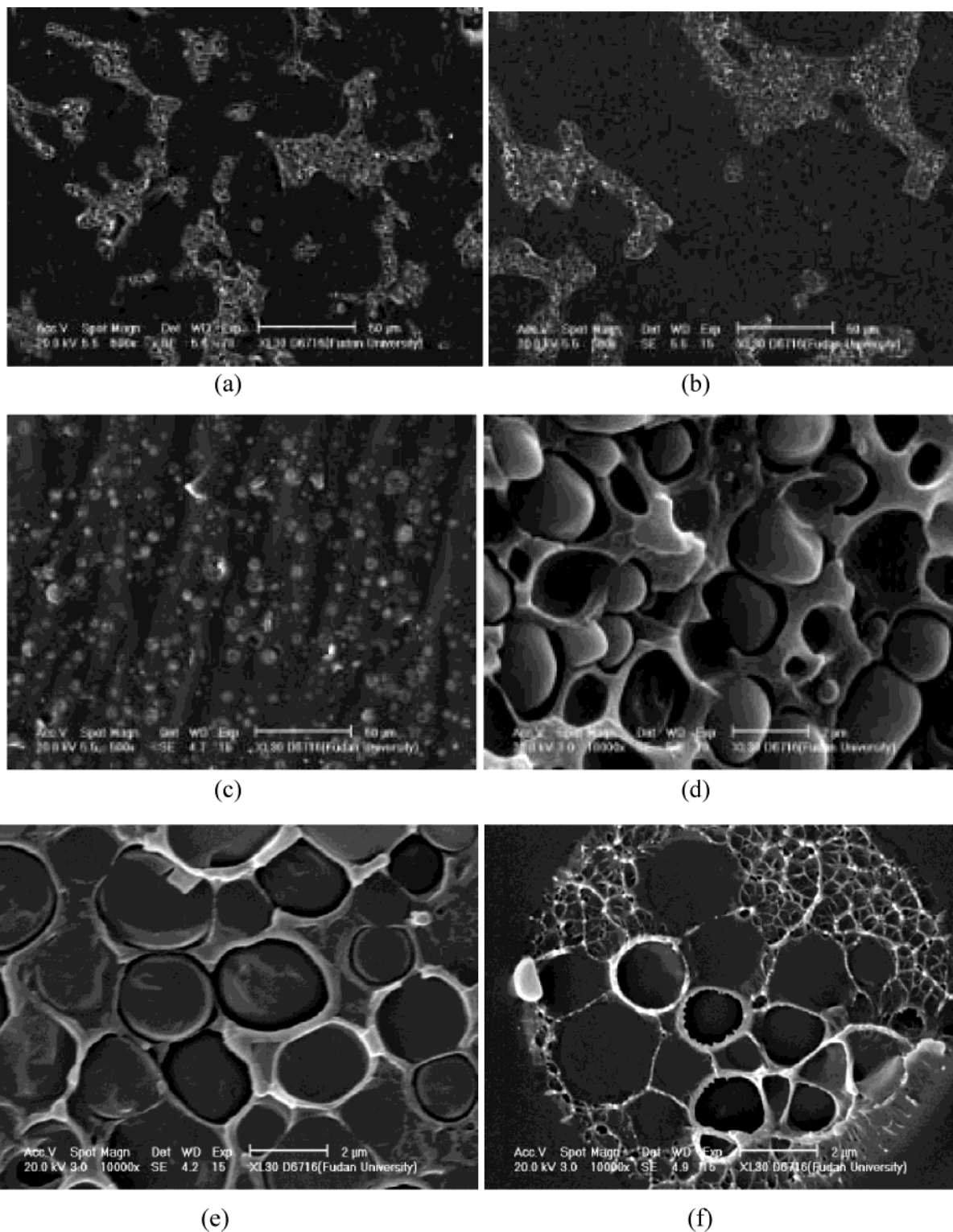


Figure 2. SEM of three blends cured at 150 °C for 5 h. (a) P720, ×500; (b) HP720, ×500; (c) NP720, ×500; (d) P720, ×10000; (e) HP720, ×10000; (f) NP720, ×10000.

the beginning of the phase separation. The appearance of the scattering peak and the continuous increase in the scattering intensity are indications of the development of a regularly phase-separated morphology via spinodal decomposition.^{29,30} We observed similar characteristics at all temperatures.

To describe the tendency of the change in q_m with time, time-dependent q_m was fit with a Maxwell-type relaxation (eq 2). The curve in Figure 3b shows that q_m decreases exponentially and fits eq 2 well.

$$q_m(t) = q_0 + A_0 \exp\left(-\frac{t}{\tau}\right) \quad (2)$$

As $t \rightarrow \infty$, $q_m = q_0$. Here, τ is the relaxation time, and A_0 is the magnifier. We notice that the values of q_m were adopted from the beginning to the first lowest value for simulation.

It is quite interesting to find that the temporal change in q_m is well described by the exponential function. However, the reason that it can be described by the

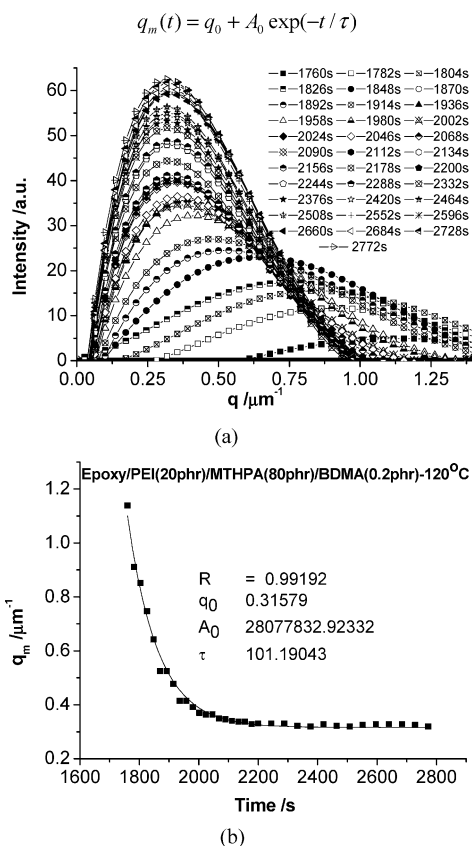


Figure 3. TRLS profiles of the P720 system cured at 120 °C. (a) Intensity versus q_m at different times and (b) q_m versus time. Symbols correspond to experimental data, and lines correspond to the fitting with eq 2.

Table 2. TRLS Results for the P720 System

temperature curing $T(^{\circ}\text{C})$	100	110	120	130	140	150
R^a	0.984	0.994	0.991	0.995	0.987	0.985
$t^b(\text{s})$	1914	1188	616	396	286	170
$q_0(\mu\text{m}^{-1})$	0.36 ^c	0.34 ^c	0.31 ^c	0.32 ^c	0.33 ^c	0.31 ^c
	0.37 ^d	0.35 ^d	0.32 ^d	0.33 ^d	0.35 ^d	0.37 ^d
$\tau(\text{s})$	243.6	177.2	101.2	71.5	50.6	31.0

^a The correlation coefficient. ^b The time interval between the onset of phase separation and morphology fixation. ^c Fitting with eq 2 to the q_m data from the TRLS experiments. ^d From TRLS experiments.

exponential function so well is not very obvious. It may provide an interesting theoretical question and should be considered in the future.

Because the cure temperature is far below the T_g of P-PEI (210 °C), the epoxy-anhydride n -mers act as a rapid dynamic phase (lower- T_g component), and P-PEI is a slow dynamic phase (higher- T_g component) and acts as a "cage effect".²³ Thus, the relaxation time τ obtained by the q_m single-exponential decay cannot be the relaxation time of P-PEI chain segments. It should be the time of escape for the epoxy-anhydride n -mers from the so-called "cage" of P-PEI by their relaxation movements.

The TRLS results of three systems at different temperatures are reported in Tables 2–4.

As shown in Tables 2–4, the time-dependent q_m fit the Maxwell-type relaxation equation very well for the three systems at different temperatures from 100 to 150 °C. This may suggest that the relaxation movement of epoxy-anhydride n -mers is a kind of viscoelastic process.

Table 3. TRLS Results for the HP720 System

temperature curing $T(^{\circ}\text{C})$	100	110	120	130	140	150
R^a	0.994	0.991	0.990	0.994	0.991	0.990
$t^b(\text{s})$	2932	1078	836	528	330	178
$q_0(\mu\text{m}^{-1})$	0.37 ^c	0.33 ^c	0.33 ^c	0.32 ^c	0.33 ^c	0.32 ^c
	0.37 ^d	0.33 ^d	0.34 ^d	0.34 ^d	0.38 ^d	0.36 ^d
$\tau(\text{s})$	301.9	204.9	138.1	84.3	54.2	34.9

^a The correlation coefficient. ^b The time interval between the onset of phase separation and morphology fixation. ^c Fitting with eq 2 to the q_m data from the TRLS experiments. ^d From TRLS experiments.

Table 4. TRLS Results for the NP720 System

temperature curing $T(^{\circ}\text{C})$	100	110	120	130	140	150
R^a	0.989	0.994	0.992	0.979	0.993	0.997
$t^b(\text{s})$	3690	1166	990	660	264	220
$q_0(\mu\text{m}^{-1})$	0.37 ^c	0.33 ^c	0.31 ^c	0.32 ^c	0.34 ^c	0.35 ^c
	0.36 ^d	0.36 ^d	0.32 ^d	0.32 ^d	0.38 ^d	0.39 ^d
$\tau(\text{s})$	532.1	292.9	193.4	96.8	60.1	37.4

^a The correlation coefficient. ^b The time interval between the onset of phase separation and morphology fixation. ^c Fitting with eq 2 to the q_m data from the TRLS experiments. ^d From TRLS experiments.

However, as presented in Tables 2–4, relaxation time τ and time interval t^a decrease drastically with the increase in temperature and become progressively less sensitive to the curing temperature. This can be attributed to the acceleration of the relaxation movement at higher temperature. The higher the temperature is, the more rapid the epoxy-anhydride n -mers escape from the cage of P-PEI and the more quickly the morphology can be fixed. Meanwhile, the relaxation time τ decreases with the increase in the amount of accelerator at same temperature, in which case the curing rate increases because of the presence of accelerator and the driving force of phase separation is thus improved. It is clear that relaxation time τ depend not only on the temperature of the curing reaction but also on the rate of the curing reaction. Thus, the results indicate that there exists some relationship between relaxation time τ and the phase separation induced by the curing reaction and that relaxation time τ is closely related to the rate of the curing reaction associated with the amount of accelerator and the curing temperature.

3.3. Fitting with the WLF Equation. The temperature superposition principle is usually used to assess the influence of temperature upon the viscoelastic properties of a system. To discuss the viscoelastic effect here, relaxation times τ at different temperatures listed in Tables 2–4 were fit with the Williams–Landel–Ferry (WLF) equation:

$$\log \frac{\tau}{\tau_s} = \frac{-C_1(T - T_s)}{C_2 + (T - T_s)}$$

For this complicated case, it is unreasonable to select T_g of the epoxy resin as the reference temperature. However, when C_1 and C_2 were selected as empirical constants 8.86 and 101.6 K, there exists a corresponding reference temperature (flow temperature of polymer chains or segments, which should be 50 K higher than T_g of the polymer) for all amorphous materials. Thus, the WLF equation can be rewritten in the following form:

$$\tau = \tau_s \exp \left[-\ln 10 \times 8.86 \times \frac{(T - T_s)}{(101.6 + (T - T_s))} \right] \quad (3)$$

In Figure 4, we find that the simulation results fit well to the experimental data for all three systems, which suggests that relaxation time τ obeys the time-temperature superposition (TTS) principle and can be described by the Williams-Landel-Ferry (WLF) equation. Then it can be suggested that the coarsening process of epoxy droplets is mainly controlled by the viscoelastic flow, as indicated by Zheng et al.²⁴

T_s and τ_s obtained from simulation results are listed in Table 5.

Furthermore, shift factors $a_T (= \tau/\tau_s)$ were calculated at various temperatures. $1/\log(a_T) - 1/(T - T_s)$ is plotted in Figure 5 for the three systems. It is obvious that the linear function undoubtedly exists.

In addition, as indicated above, when C_1 and C_2 in the WLF equation are selected as empirical constants 8.86 and 101.6 K, T_s may be about 50 K higher than T_g . Thus, to discuss the meaning of T_s and corresponding segments or polymers that exhibit viscoelastic flow, T_g of the blends of epoxy-anhydride were measured by DSC at different heating rates (Figure 6). It is reasonable to eliminate the effect of the heating rate on T_g by extrapolating the heating rate to zero. Thus, the T_g values of the three systems are 249.6 K (NP720), 248.7 K (HP720), and 248.2 K (P720).

The T_g values of epoxy-anhydride with 0.1 and 0.2 pbw accelerator at the same heating rate are almost the same and are about 15 K less than T_s fit with the WLF equation (264.1, 266.5 K). The T_g of the blend without accelerator is 1 to 2 K higher than that of the two others and about 40 K less than T_s (292.8 K). Therefore, T_s could be regarded as being about 50 K above the T_g of the epoxy-anhydride blend, and the viscoelastic behavior observed by TRLS could be attributed to the escape movement of epoxy-anhydride n -mers.

From the above analysis, according to T_s and τ_s , relaxation time τ at different temperatures can be evaluated for phase separation occurring at a very low rate because of the very poor mobility of the epoxy-anhydride n -mers, which might be undetectable within the limited observation time. Therefore, applying the TTS principle will afford us valuable information over a wide range of temperature.

3.4. Viscoelastic Effects on Phase Separation and the Final Morphologies. On the basis of the model of Tanaka,^{22,23} the viscoelastic domain deformation process can be characterized by two time scales— τ_d (characteristic time of deformation) and τ_{ts} (characteristic rheological time of the slower phase). τ_d decreases rapidly with the composition difference at first and then increases with the domain size, and τ_{ts} increases steeply with the composition difference and becomes almost constant in the late stage. Viscoelastic spinodal phase separation can thus be classified into three regimes: initial ($\tau_d > \tau_{ts}$) stage, elastic regime ($\tau_d < \tau_{ts}$) with anisotropic domain shape, and hydrodynamic regime ($\tau_d > \tau_{ts}$) with spherical domain shape.

In the present dynamic asymmetry systems in the middle and late stages of phase separation, the slower dynamic phase (P-PEI-rich phase) becomes more and more viscoelastic with the escape of epoxy-anhydride n -mers from the P-PEI-rich phase and then behaves as an elastic body. In the case of P720 and HP720, the morphologies can be fixed at this stage with the present

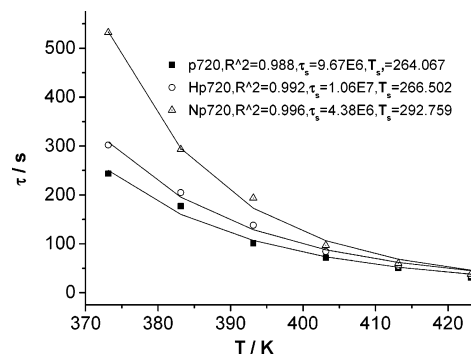


Figure 4. Plots of relaxation time τ versus temperature. Symbols correspond to experimental data, and lines correspond to the fitting with eq 3.

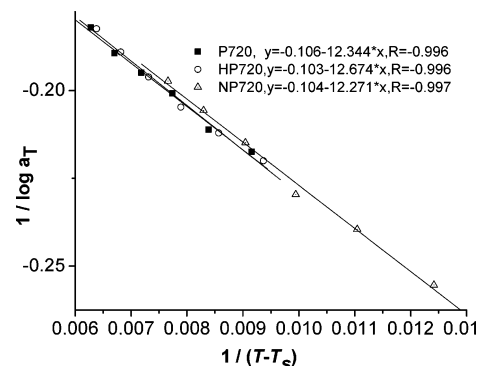


Figure 5. Plots of $1/\log a_T$ versus $1/(T - T_s)$ for three systems: P720, HP720, and NP720.

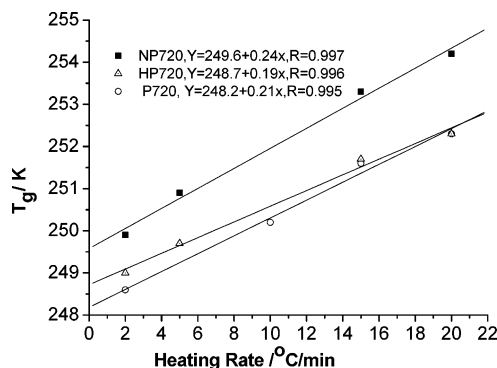


Figure 6. Glass-transition temperatures of blends of epoxy-anhydride measured by DSC at different heating rates.

Table 5. T_s and τ_s Obtained from Simulation Using Equation 3

	P720	HP720	NP720
T_s (K)	264.1	266.5	292.8
τ_s (s)	9.67×10^6	1.06×10^7	4.38×10^6

of accelerator by processes such as gelation or vitrification; the elastic force balance dominates the morphology instead of the interfacial tension, which leads to the anisotropic shape of the domain, as shown in Figure 2a and b. This may imply that the spinodal phase separations of P720 and HP720 systems are affected by viscoelastic behavior and that the final morphologies fix at the stage corresponding to the elastic regime ($\tau_d < \tau_{ts}$). In the case of NP720, the rate of the curing reaction is slow enough; the coarsening process can proceed further where the disentanglement of P-PEI chains occurs. The anisotropic shape of the domain becomes spherical again with the lowest interfacial energy because the interfacial energy overcomes the elastic

energy, as shown in Figure 2c. This may also suggest that the spinodal phase separation of the NP720 system is influenced by the viscoelastic effect and that the final morphologies fix at the stage corresponding to the hydrodynamic regime ($\tau_d > \tau_{ts}$).

Therefore, as discussed above, this suggests that the phase separation in thermoplastics-modified epoxy resin takes place according to the spinodal decomposition mechanism. In this SD phase separation, except for the thermodynamic factor, the phase separation and the final morphologies could be influenced by the kinetic factor and the viscoelastic effect associated with the dynamic asymmetry arising from the T_g difference between the components in polymer blends, resulting in various morphologies.

4. Conclusions

The results of TRLS indicate that phase separation in thermoplastics-modified epoxy resin takes place according to the spinodal decomposition mechanism and that the evolution of scattering vector q_m corresponding to the size of epoxy droplets follows the viscoelastic relaxation model. Temperature-dependent relaxation time τ obtained from $q_m(t) = q_0 + A_0 \exp(-t/\tau)$ of these systems can be described by the WLF equation. We find experimentally that the dynamical asymmetry caused by the T_g difference between the components plays an important role in the concentration fluctuations of spinodal decomposition in thermoplastics-modified epoxy. The coarsening process of epoxy droplets and the final morphologies in these thermoplastic-epoxy systems are affected by viscoelastic behavior, which is in good agreement with the viscoelastic spinodal decomposition model suggested by Tanaka and the images obtained by SEM.

Acknowledgment. This research was supported by the National Nature Science Foundation of China (grant 50273007).

References and Notes

- (1) Hedrick, J. L.; Yilgor, I.; Wilkes, G. L.; McGrath, J. E. *Polym. Bull.* **1985**, *13*, 201.
- (2) Oyanguren, P. A.; Riccardi, C. C.; Williams, R. J. J.; Mondragon, I. *Polymer* **1998**, *36*, 1349.
- (3) Bucknall, C. B.; Partridge, I. K. *Polymer* **1983**, *24*, 639.
- (4) Kim, B. S.; Chiba, T.; Inoue, T. *Polymer* **1995**, *36*, 43.
- (5) Kim, H.; Char, K. *Ind. Eng. Chem. Res.* **2000**, *39*, 955.
- (6) Bennett, G. S.; Farris, R. J.; Thompson, S. A. *Polymer* **1991**, *32*, 1637.
- (7) Bucknall, C. B.; Gilbert, A. H. *Polymer* **1989**, *30*, 215.
- (8) Hourston, D. J.; Lane, J. M. *Polymer* **1992**, *33*, 1379.
- (9) Bonnet, A.; Pascault, J. P.; Sautereau, H.; Camberlin, Y. *Macromolecules* **1999**, *32*, 8524.
- (10) Poncet, S.; Boiteux, G.; Pascault, J. P.; Sautereau, H.; Seytre, G.; Rogozinski, J.; Kranbuehl, D. *Polymer* **1999**, *40*, 6811.
- (11) Cui, J.; Yu, Y. F.; Li, S. J. J. M. S. *Pure Appl. Chem.* **1998**, *35*, 649.
- (12) Wu, X. G.; Cui, J.; Ding, Y. F.; Li, S. J.; Dong, B. Z.; Wang, J. *Macromol. Rapid Commun.* **2001**, *22*, 409.
- (13) Aoki, Y.; Tanaka, T. *Macromolecules* **1999**, *32*, 8560.
- (14) Pathak, J. A.; Colby, R. H.; Kamath, S. Y.; Kumar, S. K.; Stadler, R. *Macromolecules* **1998**, *31*, 8988.
- (15) Tanaka, H. *J. Chem. Phys.* **1995**, *103*, 2361.
- (16) Polios, I. S.; Soliman, M.; Lee, C.; Gido, S. P.; Rohr, K. S.; Winter, H. H. *Macromolecules* **1997**, *30*, 4470.
- (17) Clarke, N.; McLeish, T. C.; Pavawongsak, S.; Higgins, J. S. *Macromolecules* **1997**, *30*, 4459.
- (18) Hopkinson, I.; Myatt, M. *Macromolecules* **2002**, *35*, 5153.
- (19) Karatasos, K.; Vlachos, G.; Vlassopoulos, D.; Fytas, G.; Meier, G.; Du Chesne, A. J. *J. Chem. Phys.* **1998**, *108*, 5997.
- (20) Tanaka, H. *Macromolecules* **1992**, *25*, 6377.
- (21) Tanaka, H. *Phys. Rev. Lett.* **1993**, *71*, 3158.
- (22) Tanaka, H. *Phys. Rev. Lett.* **1996**, *76*, 787.
- (23) Tanaka, H. *J. Phys.: Condens. Matter* **2000**, *12*, R207.
- (24) Zheng, Q.; Peng, M.; Song, Y. H.; Zhao, T. J. *Macromolecules* **2001**, *34*, 8483.
- (25) Toyoda, N.; Takenaka, M.; Saito, S.; Hashimoto, T. *Polymer* **2001**, *42*, 9193.
- (26) Kostko, A. F.; Anisimov, M. A.; Sengers, J. V. *Phys. Rev. E* **2002**, *66*, 020803.
- (27) Montserrat, S.; Flaque, C.; Calafell, M.; Andreu, G.; Malek, J. *Thermochim. Acta* **1995**, *269/270*, 213.
- (28) Chen, W. J.; Shen, Z.; Huang, X.; Huang, J. *Macromol. Rapid Commun.* **1997**, *18*, 197.
- (29) Inoue, T. *Prog. Polym. Sci.* **1995**, *20*, 119.
- (30) Yang, Y.; Fujiwara, H.; Chiba, T.; Inoue, T. *Polymer* **1997**, *39*, 2745.

MA034649A